sustainability

MDPI

Article

Estimation and Analysis of Vehicle Exhaust Emissions at Signalized Intersections Using a Car-Following Model

Hongxing Zhao, Ruichun He * and Xiaoyan Jia

School of Traffic and Transportation, Lanzhou Jiaotong University, Lanzhou 730070, China
* Correspondence: tranman@163.com

Received: 17 June 2019; Accepted: 19 July 2019; Published: 23 July 2019



Abstract: A signalized intersection is a high fuel consumption and high emission node of a traffic network. It is necessary to study the emission characteristics of vehicles at signalized intersections in order to reduce vehicle emissions. In this study, the combination of a car-following model and the vehicle specific power emission model was used to estimate the vehicle emissions, including the CO_2, CO, HC, and nitric oxide (NO_X) emissions, at unsaturated signalized intersections. The results of simulations show that, under the influence of the signal light, the substantial changes in a vehicle's trajectory increase the CO_2, CO, HC, and NO_X emissions. The CO_2, CO, HC, and NO_X emissions from vehicles at signalized intersections were further analyzed in terms of signal timing, vehicle arrival rate, traffic interference, and road section speed. The results show that an increase in the signal cycle, the vehicle arrival rate, and the traffic interference amplitude result in increases in the CO_2, CO, HC, and NO_X emissions per vehicle at the intersection inbound approach, and an increase in the green signal ratio and the vehicle road section speed within a specified range has a positive significance for reducing the CO_2, CO, HC, and NO_X emissions of vehicles in the study range. The proposed method can be flexibly applied to the analysis of vehicle emissions at unsaturated signalized intersections. The obtained results provide a reference for the control and management of signalized intersections.

Keywords: exhaust emissions; signalized intersection; car-following model; vehicle specific power

1. Introduction

Rapid urban development has increased vehicle fuel consumption and emissions in traffic networks [1]. Many scholars have paid attention to this issue [2,3]. As a basic component of an urban transportation network, signalized intersections are the main points at which congestion and delays occur in the road network [4]. In urban traffic, the fuel consumption of vehicles that pass through an intersection accounts for more than half of that consumed for the total travel distance, and vehicle emissions will inevitably increase [5].

Since an intersection is a high fuel consumption and high emission area, based on certain assumptions, researchers have calculated the fuel consumption and exhaust emissions at intersections using various methods and by combining traffic models with vehicle emission models, which they use to analyze optimization measures. Liao and Machemehl [6] analyzed changes in a vehicle's speed at different signal stages, such as at the inbound approach to the intersection, in the intersection, and at the outbound approach to the intersection. According to the energy consumption rates at each signal stage, they proposed a cumulative energy consumption model for the vehicle at the intersection and studied the influence of signal timing on the vehicle's energy consumption based on the model. Considering the influence of random driving on the vehicle's fuel consumption, the optimal signal period with the minimum fuel consumption was derived [7]. Based on a vehicle's

fuel consumption rate under different working conditions, Li et al. [8] proposed a method for calculating the vehicle's fuel consumption at intersections when the vehicle is accelerating, decelerating, and idling. They established an intersection multi-objective optimization model that considers vehicle delay, fuel consumption, and exhaust emissions under the constraint of the minimum green light time of a pedestrian crossing. Liao and Machemehl [6] and Li et al. [8] modeled the fuel consumption and exhaust emissions generated by vehicles at a signalized intersection; however, the results were all achieved under overly ideal assumptions, which limit the model's applicability. In response to this problem, some scholars have combined a traffic model and vehicle fuel consumption and emissions models to analyze the fuel consumption and emissions of vehicles at signalized intersections. Lv and Zhang [9] used a combination of the VISSIM and MOVES models to study the influence of the coordinated control of adjacent intersections on vehicle exhaust emissions. They found that coordinated control and a car's arrival time have an influence on exhaust emissions. At the same time, Lv et al. [10] established an optimization model for intersection signal control parameters to reduce the total amount of emissions. Gao and Hu [11] used VISSIM to simulate the traffic flow characteristics at signalized intersections and obtained real-time vehicle data, such as the position, time, vehicle type, vehicle speed, and acceleration/deceleration, at the intersection. They imported these data into the VERSIT+ model and obtained the total amount of exhaust emissions from the vehicles at the intersection. Zhang et al. [12] combined VISSIM with the exhaust emission modeling method based on the vehicle specific power and established a microscopic exhaust emission simulation platform. Through a case study simulation, they evaluated the exhaust emissions at the intersection under two traffic control strategies, different signal timings, and different traffic flows. By combining the traffic simulation software VISSIM with vehicle fuel consumption and emission models, Lv and Zhang [9], Gao and Hu [11], and Zhang et al. [12] studied the fuel consumption and emissions of vehicles at an intersection and overcame the shortcomings of the overly ideal assumptions of the studies of Liao and Machemehl [6] and Li et al. [8]. However, due to the process's complexity and the large amount of required data processing, some inflexibility remains in this type of combination based on VISSIM and vehicle fuel consumption and emissions models for the study of traffic flows and emissions at signalized intersections. To overcome this problem, Tang et al. [13] simulated a vehicle's trajectory by combining a car-following model with the VT-Micro model and analyzed the influence of signal timing on the fuel consumption and emissions of vehicles at signalized intersections. They only analyzed the impact of signal timing on the fuel consumption and emissions of vehicles at signalized intersections, and neglected other factors, such as the vehicle arrival rate, traffic interference, and road section speed. Therefore, there remain many limitations to the study of exhaust emissions at signalized intersections. The conclusions that studies draw are often based on overly ideal assumptions or traffic simulation models, and their applicability in actual traffic control situations needs further analysis.

In this study, we select a car-following model to simulate a vehicle's trajectory at unsaturated signalized intersections, combine the car-following model with the vehicle specific power approach to estimate the vehicle's emissions, and analyze the influence of the signal timing, vehicle arrival rate, traffic interference, and road section speed on the emissions at signalized intersections. This study may help to deepen our understanding of vehicle emission characteristics at signalized intersections, and provides a simple method for further in-depth study of vehicle emissions at signalized intersections. The proposed method can be used to analyze the relationship between vehicle delay, parking rate, and vehicle emissions. It provides a theoretical reference for establishing a general model of vehicle emissions at signalized intersections.

2. Models

2.1. Car-Following Model

A car-following model is a mathematical description of the movement of a car in the same lane given a change in the state of motion of the leading car in the case of no overtaking. The corresponding

behavior of the following car that is caused by the change in the state of motion of the leading car is studied using a dynamic method. This model also constitutes a link or bridge between macroscopic traffic flow theory and the microscopic traffic flow model [14]. Car-following models have potential for wide application in the fields of microscopic traffic simulation, traffic capacity analysis, traffic safety evaluation, and self-cruise control. From the late 1950s to the early 1960s, General Motors (GM) laboratories performed a great deal of work on car-following theory, which greatly promoted basic research on car-following models, and its influence has continued to today [15,16]. Subsequently, a variety of different car-following models, based on experimental analysis and theoretical derivation, were proposed [17–25], which gradually laid a solid theoretical foundation for traffic flow analysis and control management. Jiang et al. [25] proposed the Full Velocity Difference (FVD) car-following model. Since it considers the influence of the difference in speed between the leading vehicle and the following vehicle on the following behavior, it can better describe the actual traffic flow. The FVD model equation is as follows:

$$a_n(t) = \kappa(V(\Delta x_n(t)) - v_n(t)) + \lambda \Delta v_n(t), \quad (1)$$

where $\Delta x_n(t) = x_{n-1}(t) - x_n(t)$; and $V(\bullet)$ is the optimal velocity function. Its equation is expressed as follows:

$$V(\Delta x_n(t)) = v_1 + v_2 \tanh(c_1(\Delta x_n(t) - l) - c_2). \quad (2)$$

In accordance with [24,25], we set the sensitivity parameters κ, λ, v_1, v_2, c_1, and c_2 of the FVD model to 0.41 s^{-1}, 0.5 s^{-1}, 6.75 m/s, 7.91 m/s, 0.13 m^{-1}, and 1.57, respectively, and the vehicle's average length l = 5 m.

In recent years, scholars have extensively researched the FVD model [26]. Considering that the car-following model summarizes the characteristics of many drivers and describes these characteristics mathematically, the simulation results represent the average driving behavior. In addition, we chose a variety of car-following models for analysis and comparison. The experimental results show that the results from simulations of these models are not identical with respect to the micro-characteristics of car-following behavior, but the macro-characteristics of vehicle deceleration, idling, and acceleration behavior are similar. Through an analysis of various models, we found that the FVD model is widely used in traffic flow research. Therefore, we chose the FVD model to simulate a vehicle's trajectory, and combined it with the vehicle specific power emission model to estimate and analyze the vehicle exhaust emissions at signalized intersections. It is worth noting that, in the simulation and analysis process, it is assumed that the vehicles at signalized intersections are all traditional, manually driven vehicles, and the influence of different vehicle types on the vehicle trajectory is neglected. In addition, with the development of electronic information technology, some high-end vehicles on the market have been equipped with an adaptive cruise control system. However, considering that these systems are not popular, we do not discuss them.

2.2. Emission Model Based on Vehicle Specific Power

Scholars have used the VT-Micro model [27,28] to conduct a series of studies on vehicle fuel consumption and emissions from different perspectives [29–32]. However, the VT-Micro model does not include the principles of engine operation and emissions, and the accuracy of the model depends on the resolution of the velocity–acceleration matrix. The exhaust emissions of the vehicle are directly related to the engine's output power, which, in turn, is closely related to the instantaneous speed and the acceleration/deceleration of the vehicle. The specific power method can be used to determine the exhaust emissions of motor vehicles at the micro-level because it considers such factors as the instantaneous speed and acceleration/deceleration of a vehicle [11]. The authors in [10–12,33,34] used the specific power method to evaluate vehicle exhaust emissions on the road and at an intersection.

This paper uses the specific power method to analyze the vehicle emissions at signalized intersections. The equation for calculating the specific power of a vehicle is expressed as follows [35]:

$$VSP = v(a(1+\varepsilon_i) + g \times grade + C_R g) + \frac{1}{2m}\rho_a C_D A(v_m + v)^2 v. \quad (3)$$

The authors in [35] simplified Equation (3) and provided the following equation for calculating the specific power of a light vehicle:

$$VSP = v(1.1a + 9.81grade + 0.132) + 0.000302v^3. \quad (4)$$

Since the object of this study is a vehicle at a signalized intersection, without loss of generality, let $grade = 0$ in Equation (4). Then, Equation (4) can be simplified as follows:

$$VSP = v(1.1a + 0.132) + 0.000302v^3. \quad (5)$$

In this study, we use Equation (5) to calculate the specific power of a vehicle at a signalized intersection.

Frey et al. [36] divided a light vehicle's specific power into multiple bins, each of which was called a specific power bin. By considering major vehicle parameters, such as the engine capacity and mileage, they gave the average emission rates of CO_2, CO, HC, and nitric oxide (NO_X) for different specific power bins of different types of vehicles. In the following analysis of vehicle exhaust emissions, it is assumed that the engine capacity of the vehicle is less than 3.5 L and the mileage is greater than 50,000 miles. The average emission rates of CO_2, CO, HC, and NO_X for different specific power bins of such vehicles are shown in Table 1. The CO_2, CO, HC, and NO_X emission rates in Table 1 were used to calculate and analyze the vehicle exhaust emissions.

Table 1. Average emission rates of CO_2, CO, HC, and nitric oxide (NO_X) in different specific power bins.

Number	Specific Power Bin (kW · ton −1)	Emission Rate (g/s)			
		CO_2	CO	HC	NO_X
1	$VSP < -2$	1.543686	0.011030	0.000901	0.001014
2	$-2 \le VSP < 0$	1.604406	0.008723	0.000901	0.001042
3	$0 \le VSP < 1$	1.130833	0.004682	0.000835	0.000423
4	$1 \le VSP < 4$	2.386260	0.012154	0.001027	0.001613
5	$4 \le VSP < 7$	3.210249	0.016731	0.001253	0.002638
6	$7 \le VSP < 10$	3.957732	0.023269	0.001664	0.003793
7	$10 \le VSP < 13$	4.752012	0.029322	0.002089	0.005098
8	$13 \le VSP < 16$	5.374221	0.036942	0.002332	0.006373
9	$16 \le VSP < 19$	5.940051	0.049513	0.002818	0.007664
10	$19 \le VSP < 23$	6.427506	0.063759	0.002985	0.009913
11	$23 \le VSP < 28$	7.065985	0.105380	0.003786	0.012685
12	$28 \le VSP < 33$	7.617703	0.247810	0.004573	0.014384
13	$33 \le VSP < 39$	8.322442	0.413069	0.005700	0.015967
14	$39 \le VSP$	8.475028	0.624663	0.007164	0.016717

3. Analysis of the Simulation Results

The FVD model was used to simulate the vehicle's trajectory when passing through a signalized intersection. A combination of the FVD model and the specific power emission model was used to analyze the influence of signal timing, vehicle arrival rate, traffic interference, and road section speed on the exhaust emissions of vehicles at unsaturated signalized intersections. Under normal circumstances and without considering traffic conflicts, whether for straight or turning traffic flow, a vehicle should follow the preceding vehicle through the signalized intersection, as shown in Figure 1.



Figure 1. Vehicles passing through signalized intersection in a car-following pattern.

In Figure 1, Vehicle 1 is the first vehicle to pass through the signalized intersection during the study period. Vehicles 2 to $n+1$ are the remaining vehicles that pass through the signalized intersection during the study period. O and D indicate the study range based on the stop lines at the inbound approach to the intersection. We aimed to simulate the exhaust emissions that arriving vehicles generate within the study range during the study period. To make the simulation more objective and accurate, the following simulation conditions were adopted:

(1) To make the simulation more closely resemble an actual traffic environment, we used data from the NGSIM (the Federal Highway Administration (FHWA) has been a leader in the development of traffic simulation models since the 1970s. The Traffic Analysis Tools Programme of the FHWA launched the Next Generation SIMulation (NGSIM) programme to help achieve extensive acceptance of microsimulation systems and ensure that the tools provide accurate results) project's Lankershim Boulevard dataset on the acceleration and deceleration trajectory of the non-following vehicles at the Lankershim Boulevard signalized intersection to determine the trajectory of the first vehicle that arrived in the signal cycle. The Lankershim Boulevard dataset was obtained under the auspices of the NGSIM program. The researchers in the NGSIM program collected vehicle trajectory data from Lankershim Boulevard in the Universal City neighborhood of Los Angeles, CA, on June 16, 2005. The study area consisted of three- to four-lane bidirectional arterial segments and three complete signalized intersections. The relationship between acceleration/deceleration and current speed was fitted using a quadratic function. The fitting results are as follows:

$$a_1(t)^+ = -0.0136v_1(t)^2 + 0.2584v_1(t) + 0.9820, \tag{6}$$

$$a_1(t)^- = 0.0031v_1(t)^2 - 0.1532v_1(t) - 0.6125. \tag{7}$$

The acceleration/deceleration trajectory of the first vehicle in the signal cycle can be determined based on Equations (6) and (7).

(2) Considering that this study mainly focuses on the influence of the change in speed trajectory on vehicle emissions at a signalized intersection, in order to avoid the influence of fluctuations in the road section speed on the quantitative analysis of vehicle emissions at the signalized intersection, we set the speed of all vehicles arriving at the point O in the study period at vol, and we do not permit the speed of a vehicle between the points O and D to exceed vol.

(3) The speeds and motion trajectories of all vehicles are determined by Newton's kinematics equations, which are as follows:

$$v_n(t + \Delta t) = v_n(t) + a_n(t)\Delta t, \tag{8}$$

$$x_n(t + \Delta t) = x_n(t) + v_n(t)\Delta t + 0.5a_n(t)\Delta t^2. \tag{9}$$

In Equations (8) and (9), Δt = 0.1 s, which represents the simulation time step.

(4) The time when the first car arrives at point O is set to be 0 in Figure 1. This car is the first to arrive at the stop line during the study period. The signal light turns red just when the first car arrives at the stop line, and the time interval between the 2nd and $n+1$ vehicles arriving at point O during the study period is constant when the vehicle arrival rate of inbound approach is determined.

(5) Due to the signal lights, some vehicles could decelerate, idle, or accelerate when passing through the intersection. To fully consider the influence of traffic interference on the exhaust emissions that the vehicles generate and to avoid the influence of vehicle queues on the following vehicles that

arrive, the distance between the stop line and point *O* is set to 300 m and the distance between point *D* and the stop line is set to 200 m.

(6) In order to describe different traffic conditions, we simulate a specific traffic situation by adopting parameter values that are specific to that situation, i.e., different values of the parameters *C*, η, *vol*, and *q* are set to describe different traffic situations.

According to the above-described simulation conditions, we set the parameters *T*, *C*, η, *vol*, and *q* as 1 h, 80 s, 2/3, 10 m/s and 500 pcu/h, respectively. Figure 2 shows the trajectories of all arriving vehicles between the points *O* and *D* during the study period in this traffic situation.

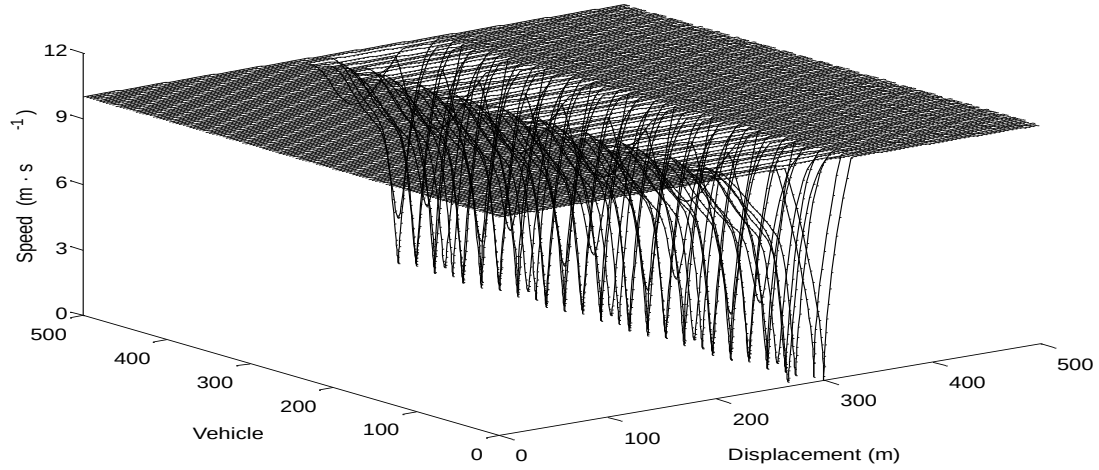

(a) Speed trajectory

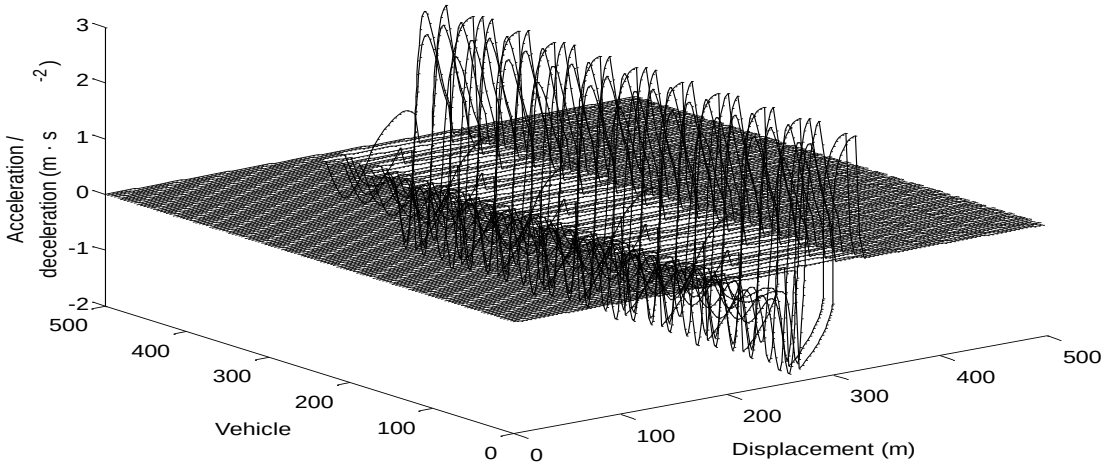

(b) Acceleration/deceleration trajectory

Figure 2. The trajectories of the arriving vehicles between points *O* and *D* during the study period.

When the vehicle arrival rate at the inbound approach is equal to 500 pcu/h, the number of vehicles that pass over the stop line during the study period is 501. Figure 2a,b shows the speed and acceleration/deceleration trajectories of all vehicles between the two points *O* and *D* based on the car-following model simulation. An analysis of the simulation results shows that some vehicles have a speed of 0 at a distance of 200–300 m from point *O*, and a small number of vehicles have a speed of less than 10 m/s. Vehicles that arrive when the light is red need to stop and wait. Vehicles that arrive at the beginning of a green light stage need to decelerate until the queuing vehicles are released. Then, they can accelerate through the signalized intersection. At the same time, as shown

in Figure 2, when a vehicle passes over the stop line, the vehicle's speed should be gradually adjusted to 10 m/s, according to the car-following model, and then maintain a constant speed. Since, in different signal cycles, the time interval between the first car's arriving at the stop line and the signal turning red is not the same, the idling time is different. If vehicles do not have exactly the same speed and acceleration/deceleration trajectories when arriving at the stop line in each cycle or the same number of vehicles pass over the stop line, differences occur in the trajectories of vehicles with different signal periods. To more clearly explain the differences in the trajectories of the vehicles arriving between the points *O* and *D* in different signal cycles, Figures 3–6 show the trajectories of the vehicles arriving at the 10th, 20th, 30th, and 40th cycles, respectively.

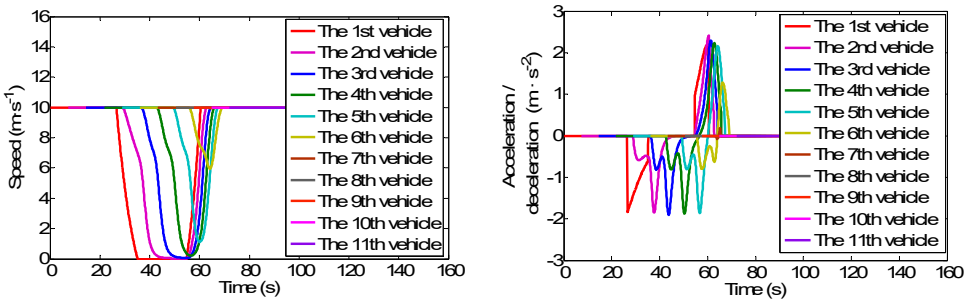

(**a**) Speed trajectory (**b**) Acceleration/deceleration trajectory

Figure 3. The trajectories of vehicles arriving in the 10th signal cycle.

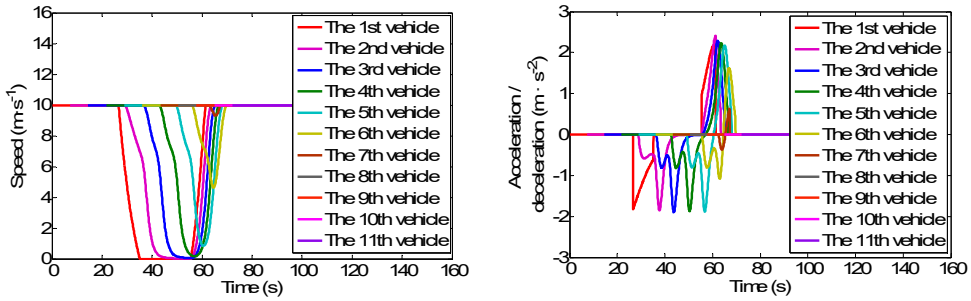

(**a**) Speed trajectory (**b**) Acceleration/deceleration trajectory

Figure 4. The trajectories of vehicles arriving in the 20th signal cycle.

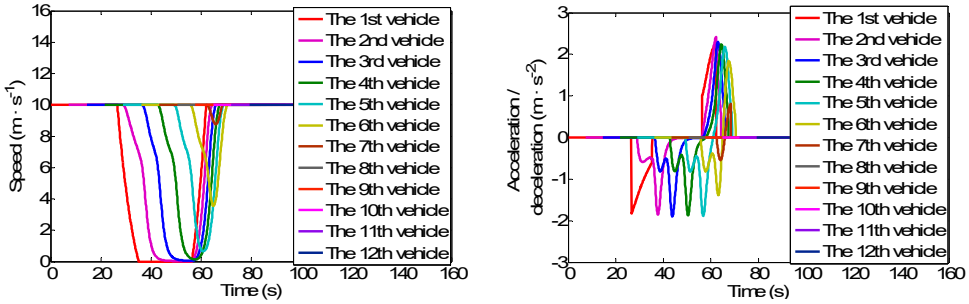

(**a**) Speed trajectory (**b**) Acceleration/deceleration trajectory

Figure 5. The trajectories of vehicles arriving in the 30th signal cycle.

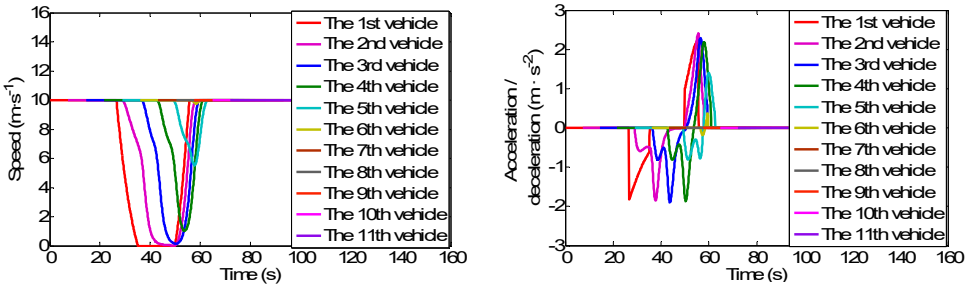

(**a**) Speed trajectory (**b**) Acceleration/deceleration trajectory

Figure 6. The trajectories of vehicles arriving in the 40th signal cycle.

In the simulation, it is assumed that the initial speed of all vehicles arriving at point *O* is 10 m/s, and the vehicle speed is no more than 10 m/s within the study range. Thus, when a vehicle's speed is equal to 10 m/s, the vehicle does not accelerate according to the car-following model. A comparison of Figures 3–6 shows that the number of vehicles that pass over the stop line in different signal cycles during the study period is not the same, and the trajectories of the arrived vehicles between point *O* and point *D* are different. This is because the time interval between the first car's arrival at the stop line and the signal becoming red is not the same in different signal cycles. The earlier the first car arrives at the stop line, the more vehicles will arrive at the stop line in this cycle. However, this could cause an increase in the idling time of the vehicles that arrive during the red light signal stage. At the same time, it can be seen from Figures 3–6 that, under the influence of the red light signal, the acceleration and deceleration of the vehicles that arrived at an earlier time in the signal cycle are larger than those that arrived at a later time.

Based on the determined trajectories of the arrived vehicles, and in combination with the specific power emission model, the CO_2, CO, HC, and NO_X emissions that the vehicles generate within the study range can be determined. Figure 7 shows the CO_2, CO, HC, and NO_X emissions that were generated by the vehicles between points *O* and *D* in the study period. Figure 8 shows the CO_2, CO, HC, and NO_X emissions per vehicle in each signal cycle.

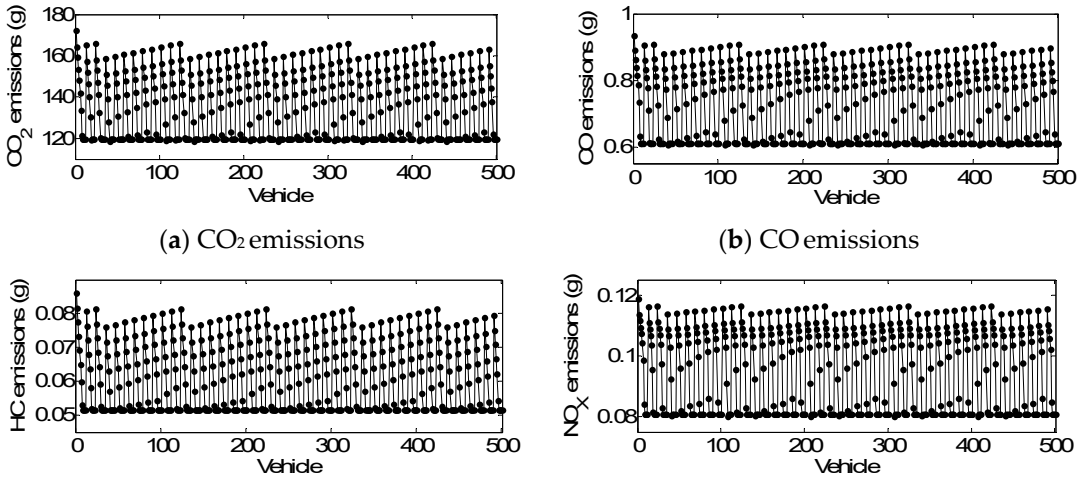

(**a**) CO_2 emissions (**b**) CO emissions

(**c**) HC emissions (**d**) NO_X emissions

Figure 7. CO_2, CO, HC, and NO_X emissions of arrived vehicles between points *O* and *D*.

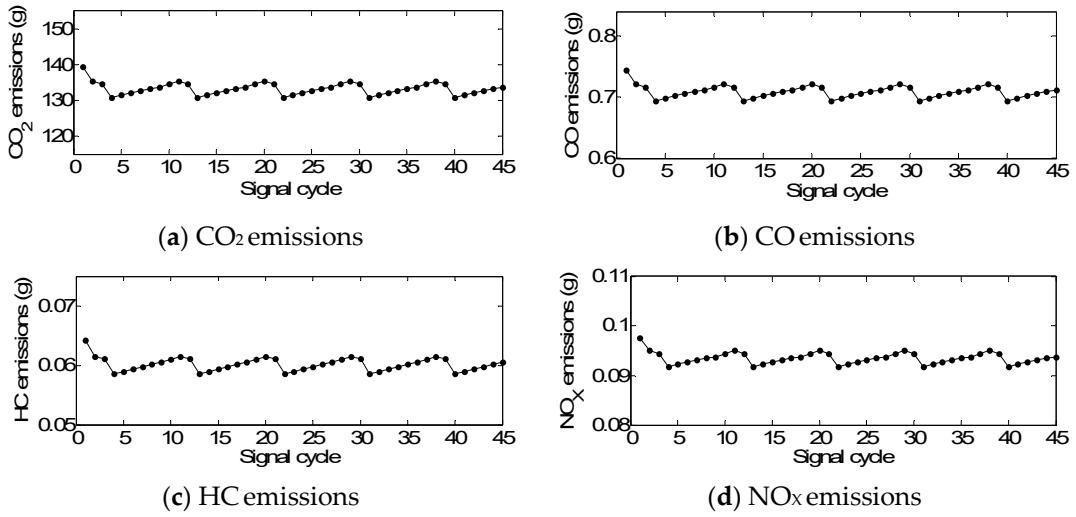

Figure 8. CO_2, CO, HC and NO_X emissions per vehicle in different signal cycles.

The following can be observed from Figures 7 and 8:

(1) The CO_2, CO, HC, and NO_X emissions generated by the arrived vehicles between points *O* and *D* within the study period are quite different. When the vehicles are affected by the red light signal and change their trajectories, the CO_2, CO, HC, and NO_X emissions are increased, and the increases are related to the idling time and the magnitude of the speed change.

(2) The CO_2, CO, HC, and NO_X emissions per vehicle in different signal cycles are close but not identical.

(3) When the vehicle trajectory is not affected between points *O* and *D* by the light signal, the CO_2, CO, HC, and NO_X emissions of the vehicles are 119.5516, 0.6089, 0.0515, and 0.0808 g, respectively. The CO_2, CO, HC, and NO_X emissions per vehicle in the study period are 133.3265, 0.7091, 0.0602, and 0.0935 g, respectively. The extent of the increase in CO_2, CO, HC, and NO_X emissions per vehicle is 11.52%, 16.46%, 16.89%, and 15.72%, respectively, due to the influence of the light signal.

Since the relative time between the first car's arrival at the stop line and the signal becoming red is not the same in different signal cycles, the number of vehicles that have arrived at the stop line in each cycle and the number of vehicles that pass through the stop line are not exactly the same, which results in differences in the CO_2, CO, HC, and NO_X emissions per vehicle during each signal cycle. Moreover, by analyzing the CO_2, CO, HC, and NO_X emissions of different vehicles in different signal cycles, it can be observed that there is a strong correlation between the CO_2, CO, HC, and NO_X emissions of the arrived vehicles in the cycle and their arrival times. Due to the influence of the red light signal, the vehicles that arrive need to decelerate and idle, and then accelerate to pass through the intersection when the light turns green. Compared with vehicles that arrive during the green light signal, they have additional idling time, deceleration and acceleration, and CO_2, CO, HC, and NO_X emissions. It is worth noting that there are a few vehicles that are affected by queuing vehicles, and there will be a very small deceleration behavior. At this time, the specific power of vehicles will be reduced, and the CO_2, CO, HC and NO_X emission rates will also be reduced correspondingly. Although, the vehicle CO_2, CO, HC, and NO_X emission rates will be increased when the vehicle accelerates, but the duration keeps very short time. As a result, the CO_2, CO, HC, and NO_X emissions of these vehicles would be slightly smaller than those of vehicles passing through intersections smoothly. To fully illustrate the influence of a vehicle's arrival time on the CO_2, CO, HC, and NO_X emissions generated between points *O* and *D* during the signal cycle, Figures 9–12 show the changes in CO_2, CO, HC, and NO_X emissions from different vehicles during the 10th, 20th, 30th, and 40th signal cycles.

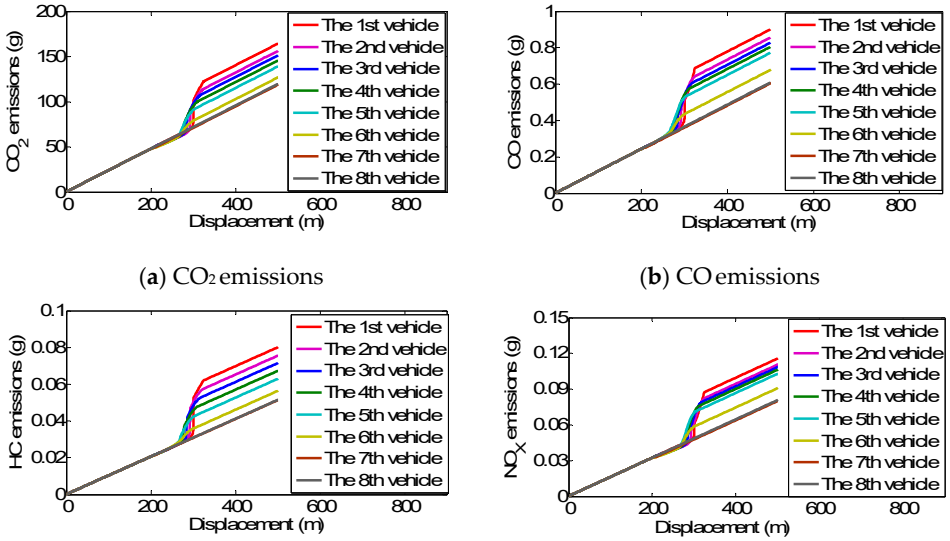

(**a**) CO_2 emissions (**b**) CO emissions

(**c**) HC emissions (**d**) NO_X emissions

Figure 9. Emissions of the vehicles that arrived in the 10th signal cycle.

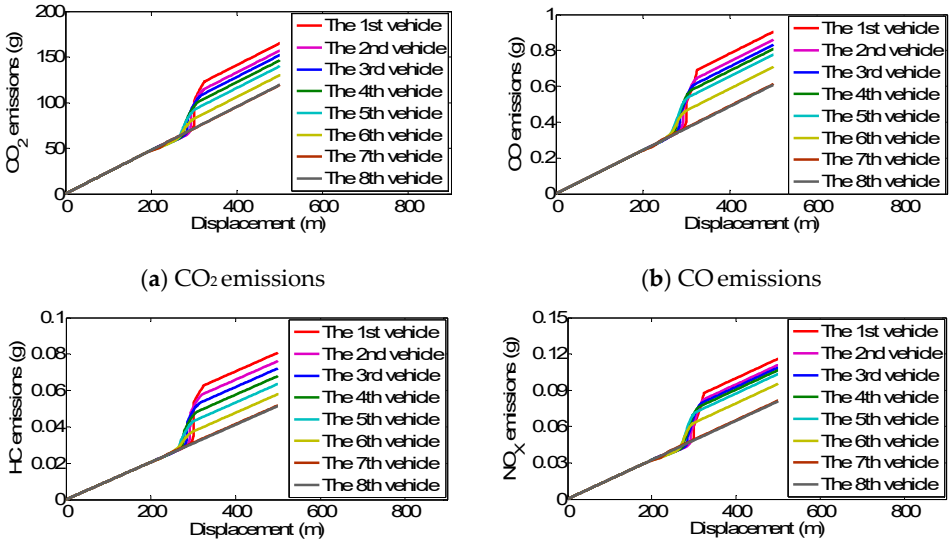

(**a**) CO_2 emissions (**b**) CO emissions

(**c**) HC emissions (**d**) NO_X emissions

Figure 10. Emissions of the vehicles that arrived in the 20th signal cycle.

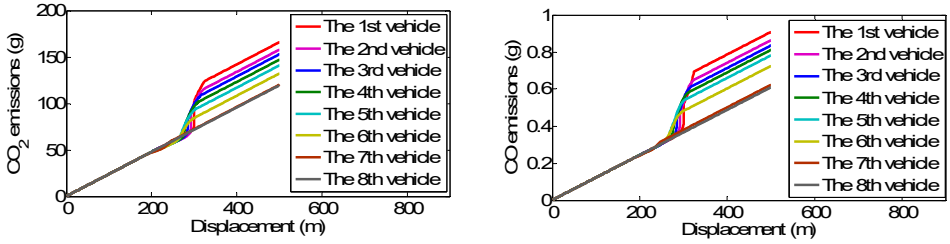

(**a**) CO_2 emissions (**b**) CO emissions

Figure 11. *Cont.*

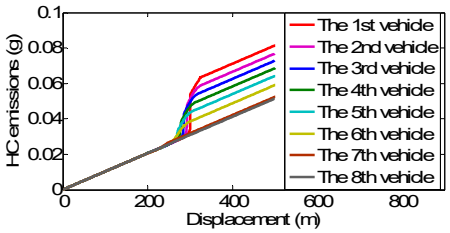

(**c**) HC emissions

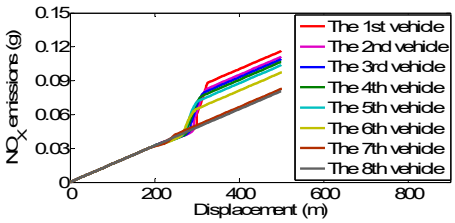

(**d**) NOx emissions

Figure 11. Emissions of the vehicles that arrived in the 30th signal cycle.

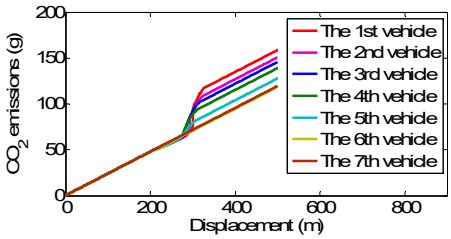

(**a**) CO_2 emissions

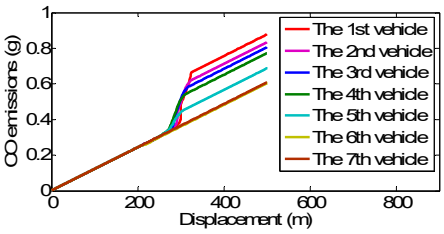

(**b**) CO emissions

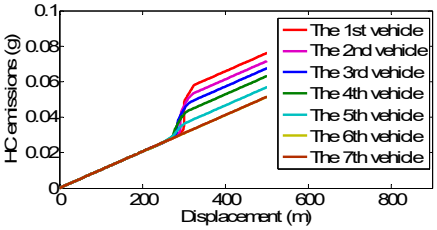

(**c**) HC emissions

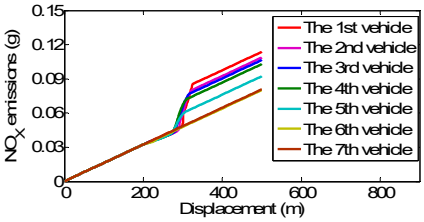

(**d**) NOx emissions

Figure 12. Emissions of the vehicles that arrived in the 40th signal cycle.

It should be noted that, in the simulation environment, vehicles after the 7th, 7th, 7th, and 6th vehicles in the 10th, 20th, 30th, and 40th signal cycles, respectively, were not affected by the light signal. Therefore, Figures 9–12 only show the CO_2, CO, HC, and NO_X emissions of the first eight, eight, eight, and seven vehicles in the 10th, 20th, 30th, and 40th signal cycles, respectively. By combining Figures 3–6 and Figures 9–12, we can obtain the following:

(1) The first six, six, six, and five vehicles in the 10th, 20th, 30th, and 40th signal cycles are affected by the light signal. These vehicles' trajectories are clearly changed, and their CO_2, CO, HC, and NO_X emissions are increased compared with those vehicles that are not affected. Although the trajectory of the 7th, 7th, 7th, and 6th vehicles in the 10th, 20th, 30th, and 40th signal cycles has changed, the range is very small; so, there is almost no difference in the CO_2, CO, HC, and NO_X emissions compared with those vehicles whose trajectory was not changed. Moreover, an analysis of the simulation showed that the deceleration process affects some vehicles, and their CO_2, CO, HC, and NO_X emissions may even be slightly reduced.

(2) In the range of 200 m from point *O*, the light signal does not affect the trajectories of the vehicles, and the CO_2, CO, HC, and NO_X emission rates of all vehicles are consistent. However, in the range of 200–300 m from point *O*, under the influence of the light signal, some vehicles need to decelerate. At this time, the specific power of the affected vehicles will be reduced, and the CO_2, CO, HC, and NO_X emission rates will be reduced correspondingly. However, due to the need to accelerate again after deceleration, and the significant increase in the vehicle's specific power during the acceleration stage, the CO_2, CO, HC, and NO_X emission rates will also increase significantly.

The analysis of the vehicle emission characteristics shows that, under acceleration and deceleration conditions, the CO_2, CO, HC, and NO_X emissions of the vehicles per unit mileage are much higher

than those at a constant speed. In combination with the analysis of the vehicles' trajectory in the signal cycle, this shows that the vehicles arriving at the beginning of the signal cycle have changed their trajectories within the range of 200–300 m from point *O*. This change has not only increased the idling time of the vehicles but also significantly increased the CO_2, CO, HC, and NO_X emissions of the vehicles due to acceleration. Therefore, the increases in CO_2, CO, HC, and NO_X emissions from the vehicles arriving at the beginning of the signal cycle are caused by deceleration, idling, and acceleration. The vehicles arriving later can pass smoothly through the intersection without increases in CO_2, CO, HC, and NO_X emissions.

Based on the above analysis, it can be seen that the increases in CO_2, CO, HC, and NO_X emissions from the vehicles at the intersection are caused by the substantial changes in the vehicles' trajectory. Therefore, considering that the trajectory of a vehicle at the intersection is affected by many factors, in the following sections we only analyze the CO_2, CO, HC, and NO_X emissions of vehicles at the intersection in terms of the signal timing, vehicle arrival rate, traffic interference, and road section speed.

3.1. Influence of Signal Timing on Exhaust Emissions

As demonstrated in the previous section, the increases in CO_2, CO, HC, and NO_X emissions from the vehicles at the intersection are due to the changes in each vehicle's trajectory. Considering that signal timing can significantly affect the delay and stopping rate of vehicles at the intersection, in this section we present a numerical simulation of the influence of signal timing on the CO_2, CO, HC, and NO_X emissions of the vehicles at the intersection.

The simulation conditions were the same as those described in Section 3. We set the parameters T, η, vol, and q as 1 h, 2/3, 10 m/s, and 500 pcu/h, respectively. The changes in the CO_2, CO, HC, and NO_X emissions of the vehicles at the intersection in the case of the signal cycle C = 50, 75, 100, 120, 150, 180, and 200 s were separately analyzed.

When the vehicle arrival rate at the inbound approach is equal to 500 pcu/h, in the case of the signal cycle C = 50, 75, 100, 120, 150, 180, and 200 s, the number of vehicles that pass over stop line in the study period is 501. Figure 13 shows the CO_2, CO, HC, and NO_X emissions of these vehicles between points *O* and *D*. Figure 14 shows the CO_2, CO, HC, and NO_X emissions per vehicle for each signal cycle. Table 2 shows the CO_2, CO, HC, and NO_X emissions per vehicle during the study period.

To more clearly compare the changes in the CO_2, CO, HC, and NO_X emissions of different vehicles, Figure 13 only lists the CO_2, CO, HC, and NO_X emissions of the first 150 vehicles. By combining Figures 13 and 14 with Table 2, we can obtain the following:

(1) When the signal cycle is extended, the vehicles that need to stop completely during the red light period have a longer idling time, and the CO_2, CO, HC, and NO_X emissions of these vehicles also increase.

(2) Due to the extension of the signal cycle, the emissions of the arrived vehicles during the red light period increase, leading to increases in the CO_2, CO, HC, and NO_X emissions per vehicle during the signal cycle.

(3) The results reveal that, under the adopted simulation conditions, the influence of the signal cycle on the number of vehicles stopped at the intersection is not obvious. In the case of the signal cycle C = 50, 75, 100, 120, 150, 180, and 200 s, the vehicle stop rate is 0.60, 0.55, 0.54, 0.52, 0.52, 0.52, and 0.51, respectively. However, the average idling time per vehicle increases significantly, resulting in increases in the CO_2, CO, HC, and NO_X emissions per vehicle during the study period. Relative the signal period is 50 s, the extent of the increase in the CO_2, CO, HC, and NO_X emissions per vehicle when the signal period is 75, 100, 120, 150, 180, and 200 s are shown in Table 3.

Based on the same green light signal ratio, the changes in CO_2, CO, HC, and NO_X emissions of the vehicles at the intersection in different signal cycles were analyzed. However, compared to the signal cycle, the green light signal ratio can also significantly affect the stopping behavior and idling time of the vehicles at the intersection. Therefore, the influence of the green light signal ratio

on the CO_2, CO, HC, and NO_X emissions of the vehicles at the intersection was further analyzed by a numerical simulation.

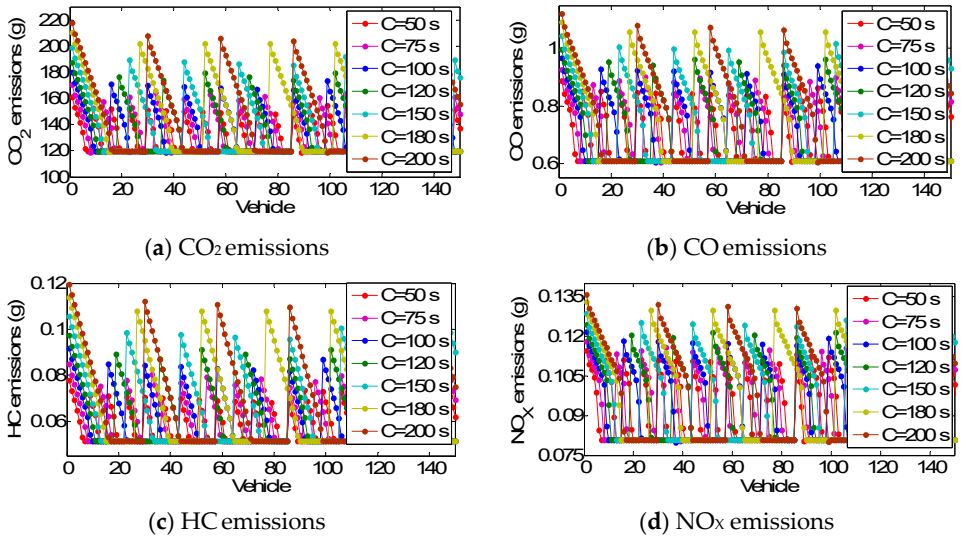

(**a**) CO_2 emissions (**b**) CO emissions

(**c**) HC emissions (**d**) NOx emissions

Figure 13. CO_2, CO, HC, and NO_X emissions of the arrived vehicles.

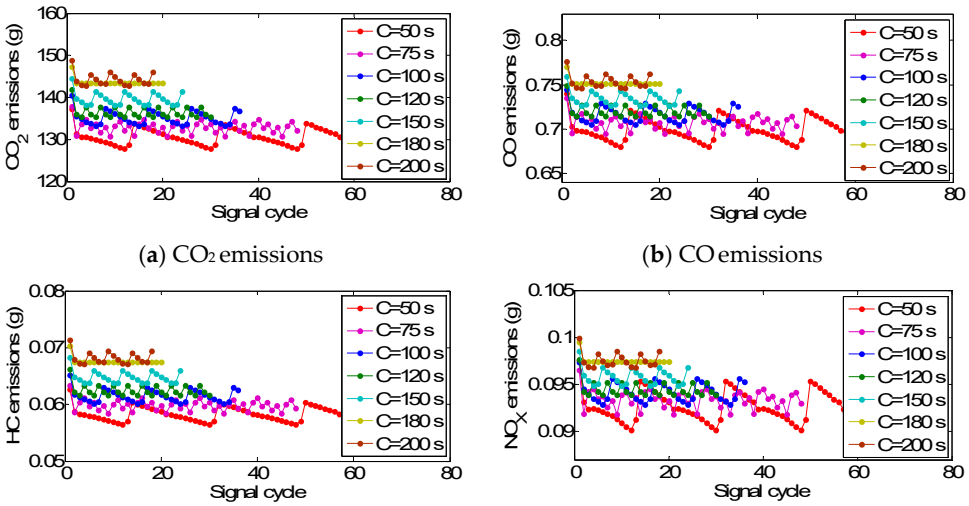

(**a**) CO_2 emissions (**b**) CO emissions

(**c**) HC emissions (**d**) NOx emissions

Figure 14. CO_2, CO, HC, and NO_X emissions per vehicle in each signal cycle.

Table 2. CO_2, CO, HC, and NO_X emissions per vehicle during the study period.

Signal Cycle (s)	Emissions (g)			
	CO_2	CO	HC	NO_X
50	130.7099	0.6994	0.0583	0.0927
75	132.9915	0.7079	0.0599	0.0934
100	135.1982	0.7166	0.0615	0.0942
120	136.5032	0.7210	0.0625	0.0946
150	139.6817	0.7346	0.0648	0.0959
180	143.6117	0.7519	0.0676	0.0975
200	144.3555	0.7539	0.0682	0.0976

Table 3. The extent of the increase in the CO_2, CO, HC, and NO_X emissions per vehicle.

Signal Cycle (s)	Extent of the Increase			
	CO_2	CO	HC	NO_X
75	1.75%	1.22%	2.74%	0.76%
100	3.43%	2.46%	5.49%	1.62%
120	4.43%	3.09%	7.20%	2.05%
150	6.86%	5.03%	11.15%	3.45%
180	9.87%	7.51%	15.95%	5.18%
200	10.44%	7.79%	16.98%	5.29%

The simulation conditions were the same as those described in Section 3. We set the parameters T, C, vol, and q as 1 h, 80 s, 10 m/s, and 500 pcu/h, respectively. Then, the changes in the CO_2, CO, HC, and NO_X emissions of the vehicles at the intersection were analyzed with the green light signal ratio η = 0.4, 0.5, 0.6, 0.7, and 0.8.

When the vehicle arrival rate at the inbound approach is equal to 500 pcu/h, in the case where the green light signal ratio η = 0.4, 0.5, 0.6, 0.7, and 0.8, the number of vehicles that pass over the stop line during the study period is 501. Figure 15 shows the CO_2, CO, HC, and NO_X emissions generated by the arrived vehicles between points O and D. Figure 16 shows the CO_2, CO, HC, and NO_X emissions per vehicle for each signal cycle. Table 4 shows the CO_2, CO, HC, and NO_X emissions per vehicle during the study period.

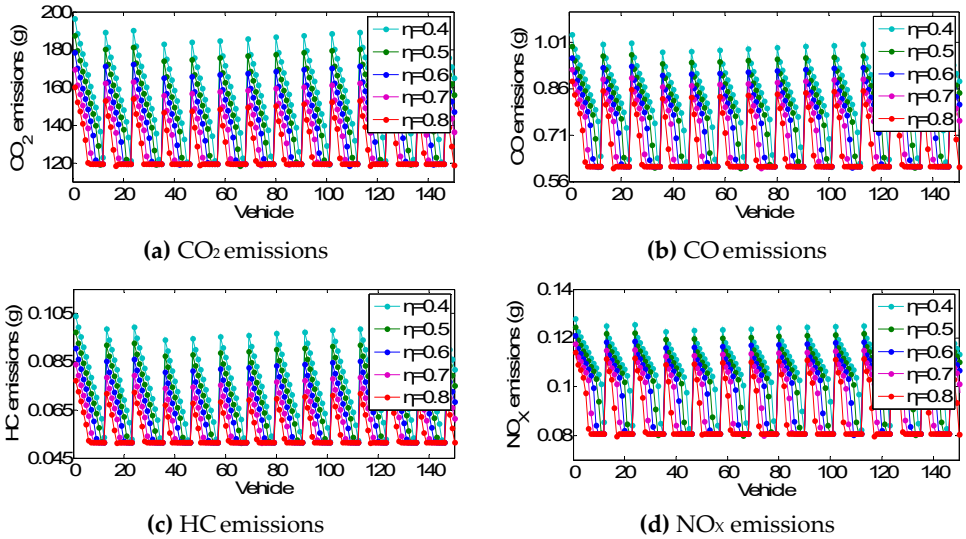

(a) CO_2 emissions **(b)** CO emissions

(c) HC emissions **(d)** NO_X emissions

Figure 15. CO_2, CO, HC, and NO_X emissions of the arrived vehicles.

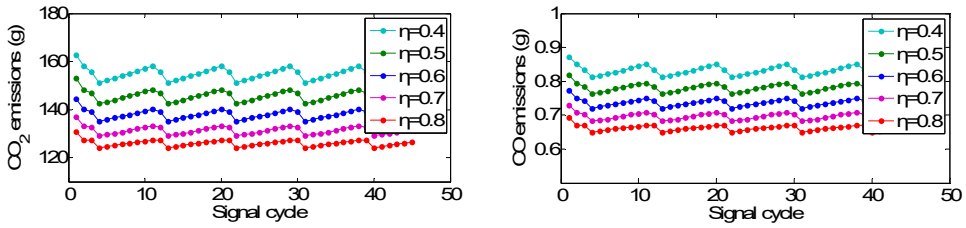

(**a**) CO_2 emissions (**b**) CO emissions

Figure 16. *Cont.*

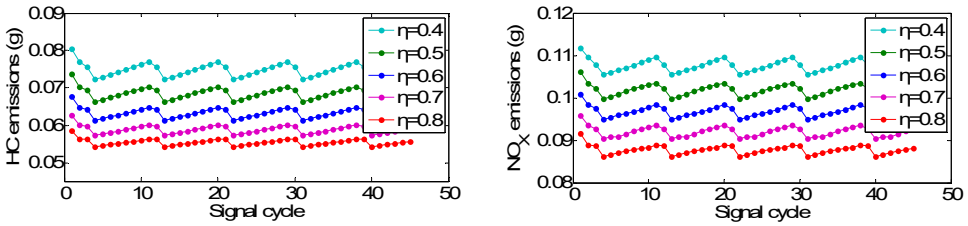

(**c**) HC emissions (**d**) NO_X emissions

Figure 16. CO_2, CO, HC, and NO_X emissions per vehicle in each signal cycle.

Table 4. CO_2, CO, HC, and NO_X emissions per vehicle during the study period.

Green Signal Ratio	Emissions (g)			
	CO_2	CO	HC	NO_X
0.4	154.8789	0.8318	0.0748	0.1076
0.5	145.6708	0.7809	0.0685	0.1018
0.6	137.9058	0.7366	0.0632	0.0968
0.7	131.3431	0.6967	0.0589	0.0920
0.8	126.0250	0.6620	0.0554	0.0878

To more clearly compare the changes in the CO_2, CO, HC, and NO_X emissions of different vehicles, Figure 15 only lists the CO_2, CO, HC, and NO_X emissions of the first 150 vehicles. By combining Figures 15 and 16 with Table 4, we can obtain the following:

(1) When the green light signal ratio is reduced, the red light time can be prolonged. The number of vehicles that need to change their trajectory, as well as the vehicle idling time, may increase during the signal cycle, resulting in an increase in CO_2, CO, HC, and NO_X emissions. These increases are relatively large.

(2) In the case where the green light signal ratio η = 0.4, 0.5, 0.6, 0.7, and 0.8, the results reveal that, under the adopted simulation conditions, with an increase in the green light signal ratio, the number of vehicles stopped at the intersection and the average vehicle idling time during the study period could be significantly reduced, possibly resulting in decreases in the CO_2, CO, HC, and NO_X emissions per vehicle in each signal cycle and during the study period. Relative the green light signal ratio is 0.4, the extent of the decrease in the CO_2, CO, HC, and NO_X emissions per vehicle when the green light signal ratio is 0.5, 0.6, 0.7 and 0.8 are shown in Table 5.

Table 5. The extent of the decrease in the CO_2, CO, HC, and NO_X emissions per vehicle.

Green Signal Ratio	Extent of the Decrease			
	CO_2	CO	HC	NO_X
0.5	5.95%	6.12%	8.42%	5.39%
0.6	10.96%	11.45%	15.51%	10.04%
0.7	15.20%	16.24%	21.26%	14.50%
0.8	18.63%	20.41%	25.94%	18.40%

The analysis of the simulation shows that, under the same simulation conditions, the signal timing has an impact on the CO_2, CO, HC, and NO_X emissions of the vehicles. When the green light signal ratio is constant, the influence of the signal cycle on the number of vehicles stopped at the intersection is not obvious, but the vehicle idling time may increase significantly, resulting in increases in the average CO_2, CO, HC, and NO_X emissions per arrived vehicle in the study period. When the signal cycle is constant, as the green light signal ratio decreases, the number of vehicles stopped at the intersection and the average vehicle idling time increase simultaneously during the study period, resulting in increases in the average CO_2, CO, HC, and NO_X emissions per arrived vehicle in the study period.

3.2. Influence of the Arrival Rate on the Exhaust Emissions

The vehicle arrival rate is another important factor that can affect the number of vehicles stopped and the vehicle idling time at the intersection. The influence of signal timing on the emissions of

vehicles at the intersection was analyzed, but the influence of the vehicle arrival rate on the emissions of vehicles at the intersection has not been analyzed. Therefore, in this section, we present an analysis of the influence of the arrival rate on the CO_2, CO, HC, and NO_X emissions of the vehicles at the intersection through a numerical simulation.

The simulation conditions were the same as those described in Section 3. We set the parameters T, C, η, and vol as 1 h, 80 s, 2/3, and 10 m/s, respectively. The changes in the CO_2, CO, HC, and NO_X emissions of the vehicles at the intersection were analyzed in the cases where the arrival rate q = 300, 400, 500, 600, 700, and 800 pcu/h.

In the case where the arrival rate of vehicles at the inbound approach to the intersection q = 300, 400, 500, 600, 700, and 800 pcu/h, the number of vehicles that passed over the stop line during the study period is 301, 401, 501, 601, 707, and 801, respectively. Figure 17 shows the CO_2, CO, HC, and NO_X emissions generated by the arrived vehicles between points O and D. Figure 18 shows the CO_2, CO, HC, and NO_X emissions per vehicle in each signal cycle. Table 6 shows the CO_2, CO, HC, and NO_X emissions per vehicle in the study period.

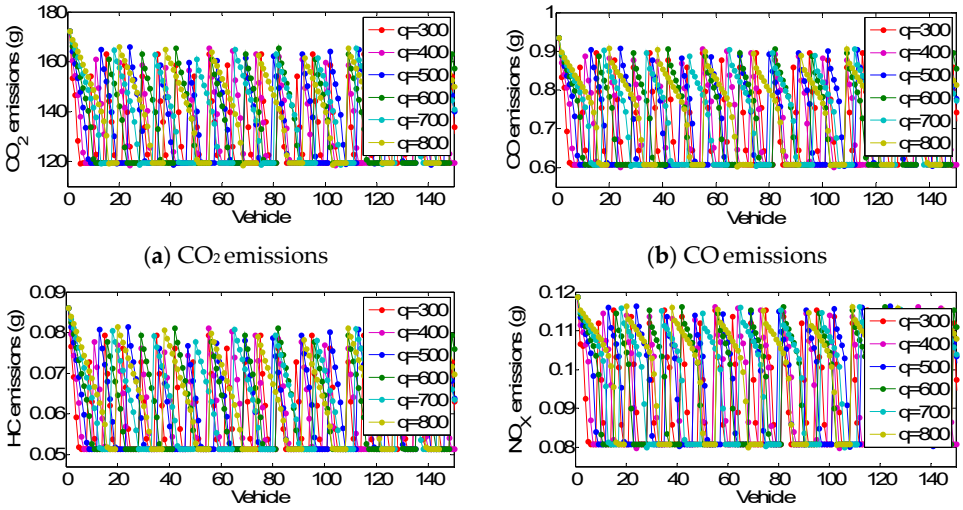

(**a**) CO_2 emissions (**b**) CO emissions

(**c**) HC emissions (**d**) NO_X emissions

Figure 17. CO_2, CO, HC, and NO_X emissions of the arrived vehicles.

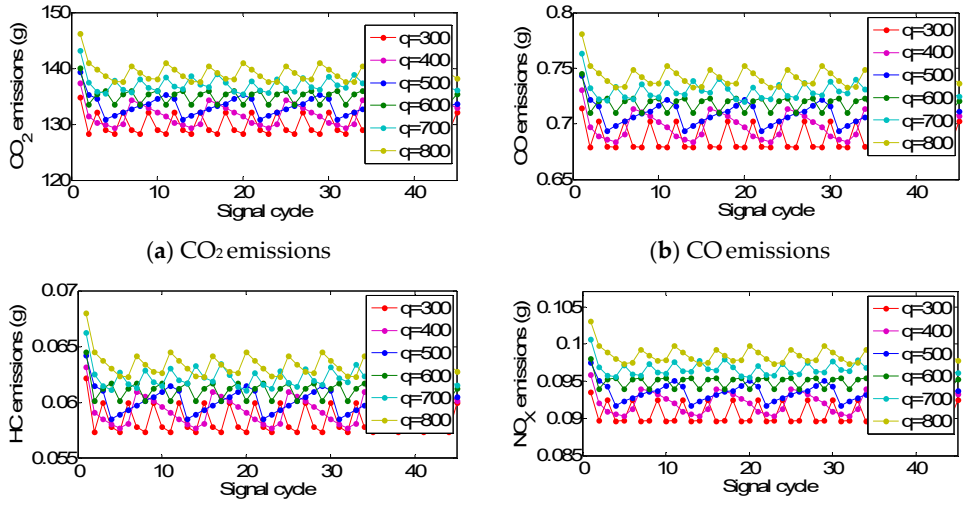

(**a**) CO_2 emissions (**b**) CO emissions

(**c**) HC emissions (**d**) NO_X emissions

Figure 18. CO_2, CO, HC, and NO_X emissions per vehicle in each signal cycle.

Table 6. CO_2, CO, HC, and NO_X emissions per vehicle during the study period.

Arrival Rate (pcu/h)	Emissions (g)			
	CO_2	CO	HC	NO_X
300	130.0280	0.6884	0.0586	0.0908
400	131.7347	0.6986	0.0593	0.0922
500	133.3265	0.7091	0.0602	0.0935
600	135.1052	0.7186	0.0611	0.0950
700	137.0340	0.7294	0.0622	0.0966
800	139.1663	0.7419	0.0634	0.0984

It should be noted that, in the cases of different arrival rates, the number of vehicles that passed over the stop line in the study period is different. To more clearly compare the changes in the CO_2, CO, HC, and NO_X emissions of different vehicles, Figure 17 only lists the CO_2, CO, HC, and NO_X emissions of the first 150 vehicles. By combining Figures 17 and 18 with Table 6, we can obtain the following:

(1) The trajectory and idling time of the first vehicle to arrive at the stop line within the signal cycle is not be affected by the increase in arrival rate, and its CO_2, CO, HC, and NO_X emissions do not increase.

(2) As the arrival rate of the vehicles at the inbound approach increases, the number of vehicles that pass over the stop line increases during the signal cycle, and the number of vehicles that the red light signal affects also increases, resulting in increases in the CO_2, CO, HC, and NO_X emissions of these vehicles.

(3) With the increase in the arrival rate, the CO_2, CO, HC, and NO_X emissions of the vehicles in each cycle of the study period show a general increasing trend;

(4) With the increase in the vehicle arrival rate, the vehicle stop rate at the inbound approach (complete stopping and incomplete stopping) and the average vehicle idling time increase simultaneously during the study period, resulting in increases in the average CO_2, CO, HC, and NO_X emissions per vehicle in the study period. Relative the vehicle arrival rate is 300 pcu/h, the extent of the increase in the CO_2, CO, HC, and NO_X emissions per vehicle when the vehicle arrival rate is 400, 500, 600, 700, and 800 pcu/h are shown in Table 7.

Table 7. The extent of the increase in the CO_2, CO, HC, and NO_X emissions per vehicle.

Arrival Rate (pcu/h)	Extent of the Increase			
	CO_2	CO	HC	NO_X
400	1.31%	1.48%	1.19%	1.54%
500	2.54%	3.01%	2.73%	2.97%
600	3.90%	4.39%	4.27%	4.63%
700	5.39%	5.96%	6.14%	6.39%
800	7.03%	7.77%	8.19%	8.37%

3.3. Influence of Traffic Interference on the Exhaust Emissions

At a signalized intersection, the arrival and departure of vehicles could be interfered with by external factors, such as the traffic flow, nonmotorized vehicles, and pedestrians moving in different directions. At this time, a vehicle should decelerate to avoid the occurrence of accidents. In this case, the trajectory of the following vehicle is also inevitably affected by the change in the preceding vehicle's trajectory, and additional deceleration and acceleration behaviors are generated. Based on the previous analyses, the deceleration and acceleration behaviors of the vehicles are the causes of the increase in CO_2, CO, HC, and NO_X emissions. Therefore, in this section, we provide an analysis of the influence of traffic interference on the CO_2, CO, HC, and NO_X emissions of vehicles at the intersection through a numerical simulation.

Due to the complexity of traffic interference at signalized intersections, it is difficult to analyze all traffic interference phenomena using the method proposed in this paper. Considering that bicycle

interference with vehicle traffic flow is common at signalized intersections, we only analyze this kind of interference scenario. We assume that, when a bicycle and a motor vehicle are moving in the same direction, the speed of the motor vehicle will inevitably be affected when the lane is adjacent. In this case, the vehicle will first decelerate and then accelerate again after decelerating to a certain speed. In an actual traffic network, interference with traffic may occur for any vehicle within the signal cycle. The analysis methods adopted the same way in this study treat the different vehicles under traffic interference conditions. Therefore, to simplify the analysis, we only simulated the first vehicle in the signal cycle when it is affected by traffic interference. Moreover, in the analysis, when traffic interference affects a vehicle, it is assumed that the vehicle decelerates at –2 m/s^2 from its current speed with the magnitude of decrease ε, and then accelerates again according to Equation (6). The speed trajectory of the following vehicle was determined according to the car-following model.

The simulation conditions were the same as those described in Section 3. We set the parameters T, C, η, vol, and q as 1 h, 80 s, 2/3, 10 m/s, and 500 pcu/h, respectively. We assumed that the first vehicle is affected by traffic interference when it accelerates to 320 m from point O, and that the magnitudes of decrease ε are 1, 3, 5, and 7 m/s, respectively. The changes in CO_2, CO, HC, and NO_X emissions of the vehicles when subject to different traffic interference were then analyzed.

When the vehicle arrival rate at the inbound approach is equal to 500 pcu/h, in the case of a magnitude of ε = 1, 3, 5, and 7 m/s, the number of vehicles that passed over the stop line in the study period is 501. Figure 19 shows the CO_2, CO, HC, and NO_X emissions generated by the arrived vehicles between points O and D. Figure 20 shows the CO_2, CO, HC, and NO_X emissions per vehicle in each signal cycle. Table 8 shows the CO_2, CO, HC, and NO_X emissions per vehicle during the study period.

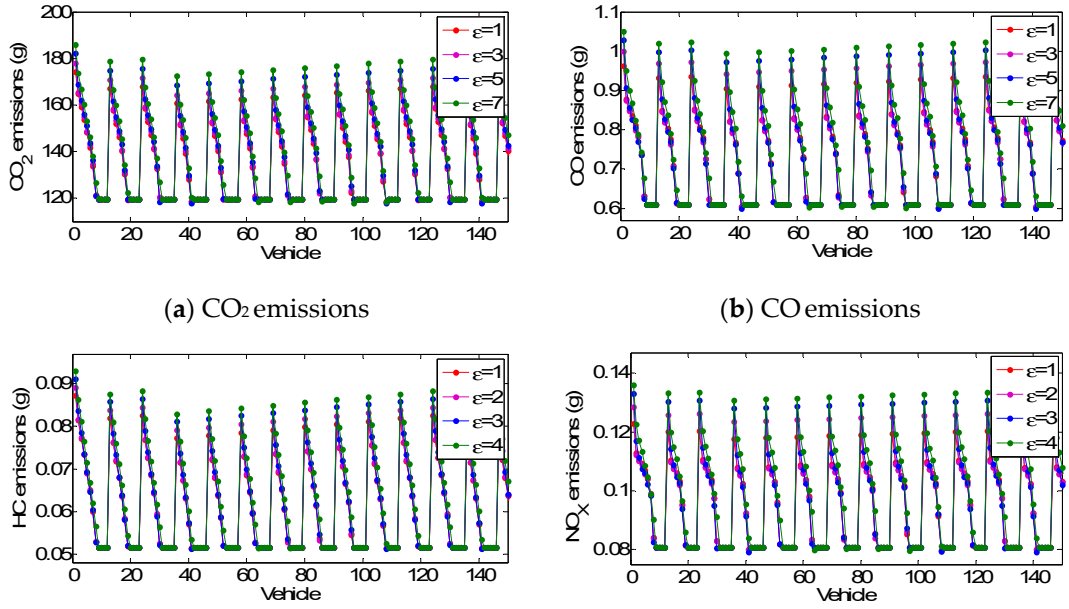

(**a**) CO_2 emissions (**b**) CO emissions

(**c**) HC emissions (**d**) NO_X emissions

Figure 19. CO_2, CO, HC, and NO_X emissions of the arrived vehicles.

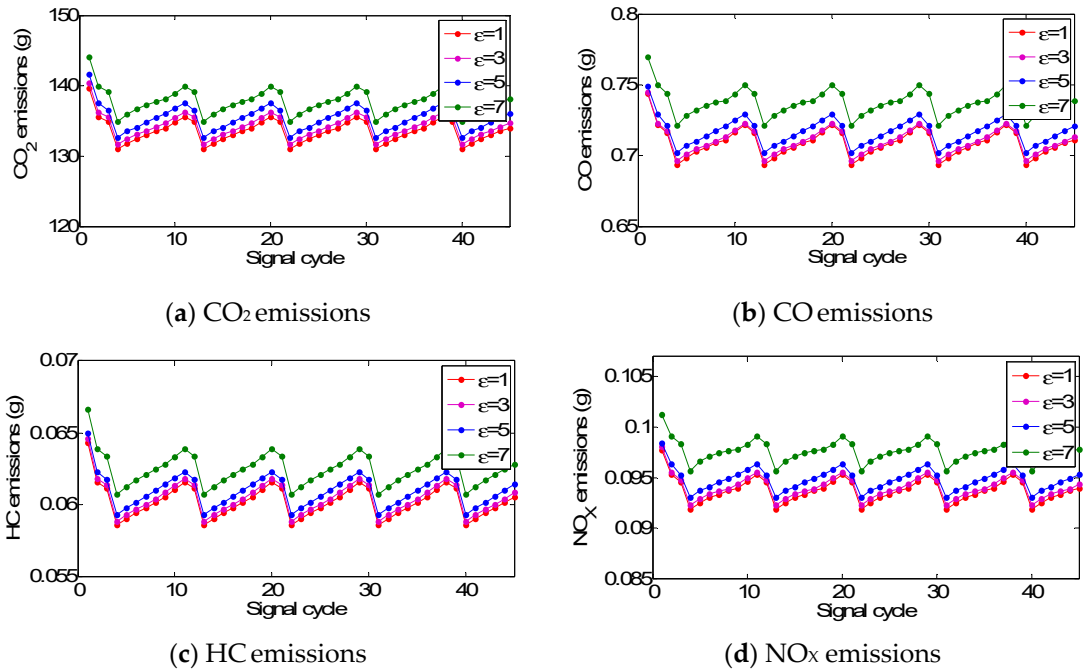

(**a**) CO_2 emissions (**b**) CO emissions

(**c**) HC emissions (**d**) NO_X emissions

Figure 20. CO_2, CO, HC and NO_X emissions per vehicle in each cycle.

Table 8. CO_2, CO, HC, and NO_X emissions per vehicle during the study period.

Magnitude of Decrease (m/s)	Emissions (g)			
	CO_2	CO	HC	NO_X
1	133.5855	0.7090	0.0602	0.0937
3	134.2548	0.7108	0.0605	0.0940
5	135.4053	0.7170	0.0610	0.0948
7	137.7570	0.7374	0.0625	0.0976

To more clearly compare the changes in CO_2, CO, HC, and NO_X emissions of different vehicles, Figure 19 only lists the CO_2, CO, HC, and NO_X emissions of the first 150 vehicles. By combining Figures 19 and 20 with Table 8, we can obtain the following:

(1) When the first vehicle in the signal cycle is affected by traffic interference, the trajectories of the following vehicles are also affected, and, as the magnitude of the decrease increases, the number of affected vehicles also increases. As the affected vehicles need to accelerate again, the CO_2, CO, HC, and NO_X emissions of the affected vehicles will increase significantly, except for a few vehicles.

(2) When the first vehicle in the signal cycle is affected by traffic interference, the CO_2, CO, HC, and NO_X emissions of the vehicles with changed trajectories decrease sequentially according to the arrival order of the vehicles.

(3) When increasing the amount of traffic interference that the first vehicle in the cycle experiences, the CO_2, CO, HC, and NO_X emissions of the vehicles at the intersection generally show an increasing trend, and the greater the traffic interference, the greater the increases in the CO_2, CO, HC, and NO_X emissions. Relative the magnitude of decrease is 1 m/s, the extent of the increase in the CO_2, CO, HC, and NO_X emissions per vehicle when the magnitude of decrease is 3, 5, and 7 m/s are shown in Table 9.

Table 9. The extent of the increase in the CO_2, CO, HC, and NO_X emissions per vehicle.

Magnitude of Decrease (m/s)	Extent of the Increase			
	CO_2	CO	HC	NO_X
3	0.50%	0.25%	0.50%	0.32%
5	1.36%	1.13%	1.33%	1.17%
7	3.12%	4.01%	3.82%	4.16%

3.4. Influence of Road Section Speed on the Exhaust Emissions

In Sections 3.1–3.3, we analyzed the effects of signal timing, vehicle arrival rate, and traffic interference on vehicle emissions at a signalized intersection, respectively. However, the foregoing simulation was based on the premise of a road section speed vol = 10 m/s. Considering that the road section speed can affect the deceleration and acceleration trajectory of a vehicle near the stop line, as well as the time that the vehicle takes to travel from point O to point D, in this section we analyze the influence of road section speed on the CO_2, CO, HC, and NO_X emissions of vehicles at the intersection using a numerical simulation.

The simulation conditions were the same as those described in Section 3. We set the parameters T, C, η, and q as 1 h, 80 s, 2/3, and 500 pcu/h, respectively. Then, we analyzed the changes in the CO_2, CO, HC, and NO_X emissions of the vehicles at the intersection in the cases of the road section speed vol = 10, 11, 12, 13, and 14 m/s.

When the vehicle arrival rate at the inbound approach is equal to 500 pcu/h, in the case where the road section speed vol = 10, 11, 12, 13, and 14 m/s, the number of vehicles that passed over the stop line during the study period is 501. Figure 21 shows the CO_2, CO, HC, and NO_X emissions generated by the arrived vehicles between points O and D. Figure 22 shows the CO_2, CO, HC, and NO_X emissions per vehicle in each signal cycle. Table 10 shows the CO_2, CO, HC, and NO_X emissions per vehicle in the study period.

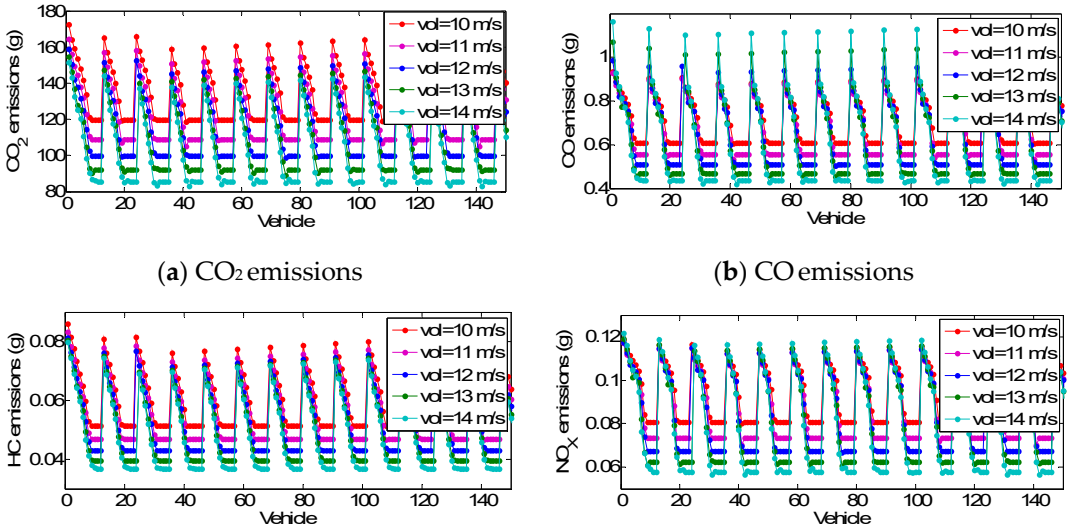

(**a**) CO_2 emissions (**b**) CO emissions

(**c**) HC emissions (**d**) NO_X emissions

Figure 21. CO_2, CO, HC, and NO_X emissions of the arrived vehicles.

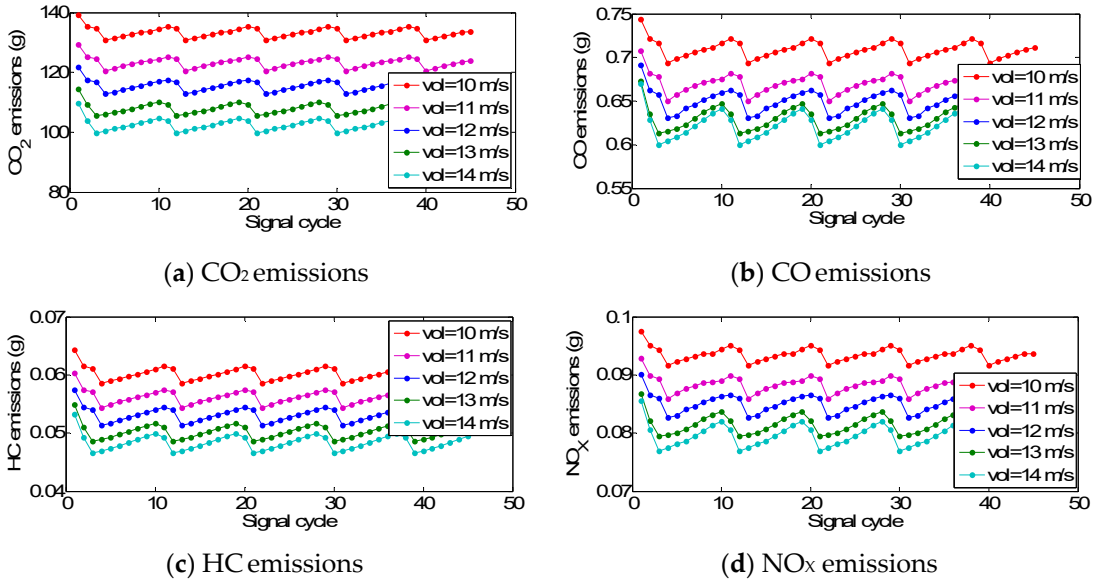

(**a**) CO_2 emissions (**b**) CO emissions

(**c**) HC emissions (**d**) NO_X emissions

Figure 22. CO_2, CO, HC, and NO_X emissions per vehicle in each cycle.

Table 10. CO_2, CO, HC, and NO_X emissions per vehicle during the study period.

vol (m/s)	Emissions (g)			
	CO_2	CO	HC	NO_X
10	133.3265	0.7091	0.0602	0.0935
11	123.2602	0.6695	0.0562	0.0884
12	115.5130	0.6496	0.0531	0.0850
13	107.9181	0.6297	0.0503	0.0815
14	102.4720	0.6211	0.0484	0.0795

To more clearly compare the changes in the CO_2, CO, HC, and NO_X emissions of different vehicles, Figure 21 only lists the CO_2, CO, HC, and NO_X emissions of the first 150 vehicles. By combining Figures 21 and 22 with Table 10, we can obtain the following:

(1) The duration of deceleration and acceleration at signalized intersections will increase as the road section speed increases. Due to the prolongation of the deceleration and acceleration processes, the CO_2, CO, HC, and NO_X emissions of the vehicles generated during the speed change will also increase, it will even increase the CO_2, CO, HC, and NO_X emissions that generated within the study range of some vehicles, and the increase of CO and NO_X is more obvious.

(2) With the increase of road section speed, the CO_2, CO, HC, and NO_X emissions of the vehicles generated during the speed change increase, but the time the vehicles take to travel between points *O* and *D* decreases, which will reduce the CO_2, CO, HC, and NO_X emissions of the vehicles generated between points *O* and *D*. The results show that, for both a single signal cycle and the whole study period, an increase in the vehicle road section speed within a specified range has a positive significance for reducing the CO_2, CO, HC, and NO_X emissions of vehicles in the study range. Relative the road section speed is 10 m/s, the extent of the decrease in the CO_2, CO, HC, and NO_X emissions per vehicle when the road section speed is 11, 12, 13, and 14 m/s are shown in Table 11.

Table 11. The extent of the decrease in the CO_2, CO, HC, and NO_X emissions per vehicle.

vol (m/s)	Extent of the Decrease			
	CO_2	CO	HC	NO_X
11	7.55%	5.58%	6.64%	5.45%
12	13.36%	8.39%	11.79%	9.09%
13	19.06%	11.20%	16.45%	12.83%
14	23.14%	12.41%	19.60%	14.97%

4. Conclusions and Discussion

In this study, the trajectories of the vehicles at signalized intersections were simulated according to the FVD model, the vehicle specific power approach was used to estimate the vehicle emissions, and the factors that influence vehicle emissions at signalized intersections were further analyzed in terms of the signal timing, vehicle arrival rate, traffic interference, and road section speed. Our conclusions can be summarized as follows:

(1) Under a certain green light signal ratio, the influence of the signal cycle on the vehicle stop rate is not obvious, but the extension of the signal cycle increases the vehicle idling time, resulting in increases in the CO_2, CO, HC, and NO_X emissions per vehicle at the intersection. This means that, when optimizing intersection timing from the perspective of vehicle emissions, vehicle delay will be a factor that has to be taken into account. If signal timing is carried out at intersections with vehicle stop rate as the only evaluation index, a larger signal cycle will increase the amount of unnecessary idle time, thus increasing the CO_2, CO, HC, and NO_X emissions.

(2) In the case of a certain signal cycle, the green light signal ratio has a greater impact on the stopping rate and the idling time of vehicles at the intersection. When the green light signal ratio is small, the CO_2, CO, HC, and NO_X emissions of the vehicles at the intersection are high. As the green light signal ratio increases, the CO_2, CO, HC, and NO_X emissions gradually decrease. Therefore, under the premise that signalized intersections contain multiple inbound approaches, it is necessary to optimize the green light signal ratio for different phases, based on a comprehensive consideration of different inbound approaches, to effectively balance the traffic time at different inlets and reduce the average vehicle emissions of the entire intersection. At the same time, considering that pedestrians need to be able to pass through intersections, the green light signal ratio of each phase should not be too large or too small, and the conditions of the minimum green light duration should be satisfied.

(3) The vehicle arrival rate has a clear influence on the CO_2, CO, HC, and NO_X emissions of the vehicles at the intersection. On the premise that the inbound approach is unsaturated, as the vehicle arrival rate increases, the stopping rate and the average idling time per vehicle increase simultaneously, resulting in increases in the CO_2, CO, HC, and NO_X emissions. As the traffic flow of urban intersections changes with time, this conclusion means that the management of signal timing in signalized intersections should be considered comprehensively according to the traffic flow of the intersections, and each intersection's timing scheme should be adjusted flexibly according to the traffic flow during different periods.

(4) Vehicles that arrive at the intersection may face interference by external factors, such as the traffic flow, nonmotorized vehicles, and pedestrians moving in different directions. In such cases, the CO_2, CO, HC, and NO_X emissions of the vehicles at the intersection may be affected by traffic interference. Therefore, when managing intersections from the perspective of vehicle emissions, it is necessary to optimize each intersection's infrastructure. The optimization of road planning can help to avoid nonmotorized vehicles interfering with motor vehicles, which is of positive significance to reduce vehicle emissions at intersections.

(5) When the urban road section speed is increased, the CO_2, CO, HC, and NO_X emissions of the vehicles generated during the speed change increase. However, from a global point of view, an increase in vehicle speed can shorten the driving time of the vehicle, which will reduce the CO_2, CO, HC, and NO_X emissions generated by the vehicle. Therefore, in urban traffic management, on the premise of ensuring traffic safety, increasing the road section speed of vehicles within a specific range may reduce the CO_2, CO, HC, and NO_X emissions of vehicles in the course of driving.

This study combined a car-following model with the vehicle specific power emission model to estimate the vehicle emissions at unsaturated signalized intersections. By analyzing the effects of signal timing, vehicle arrival rate, traffic interference, and road section speed on vehicle emissions, some meaningful conclusions were obtained. Compared with the inductive reasoning method used in previous studies, the proposed method overcomes the shortcomings of assumptions that are overly ideal. Additionally, compared with the use of simulation software, the analysis and implementation

process proposed in this paper is more simple and flexible. It can be applied in in-depth studies of vehicle emissions at signalized intersections, for example, by analyzing the relationship between vehicle delay, parking rate, and vehicle emissions. The proposed method may help to establish a general model of vehicle emissions at signalized intersections. Nevertheless, this study has some shortcomings. In order to simplify the analysis, we assumed that the interval of arrival of all vehicles is consistent, which prohibited us from fully describing the actual traffic phenomenon. In view of this deficiency, in future research, we will consider randomness in vehicle arrivals, so that the proposed method can be better applied to the analysis of actual traffic environments.

Author Contributions: The author H.Z. analyzed the simulation results and drafted the original manuscript. R.H. supervised the manuscript. X.J. polished the writing to make the paper more perfect.

Funding: This research received no external funding.

Acknowledgments: The work described in this paper was fully supported by the National Nature Science Foundation of China (No.61064012 and No.61364026). Any opinions, findings, conclusions, or recommendations expressed in this paper do not reflect the views of the Government of the China for the Innovation and Technology Support Program of the Innovation and Technology Fund.

Conflicts of Interest: The authors declare that they have no conflicts of interest.

Nomenclature

$a_n(t)$	the acceleration/deceleration of the n-th car at time t (m/s^2)
$x_n(t)$	the displacement of the n-th car at time t (m)
$\Delta x_n(t)$	the distance headway between the n-th car and its leading car n−1 at time t (m)
$v_n(t)$	the velocity of the n-th car at time t (m/s)
$\Delta v_n(t)$	the velocity difference between the n-th car and its leading car n−1 at time t (m/s)
κ	the parameter of the car-following model (s $^{-1}$)
λ	the parameter of the car-following model (s $^{-1}$)
$l = 5$	the vehicle's average length (m)
v_1	the parameter of the car-following model (m/s)
v_2	the parameter of the car-following model (m/s)
c_1	the parameter of the car-following model (m $^{-1}$)
c_2	the parameter of the car-following model
VSP	the vehicle specific power (kW $\cdot$ ton $^{-1}$)
m	the vehicle's average mass (kg)
v	the vehicle velocity (m/s)
a	the vehicle acceleration/deceleration (m/s^2)
ε_i	the mass factor
C_R	the coefficient of rolling resistance
C_D	the aerodynamic drag coefficient
A	the frontal area of the vehicle (m^2)
$grade$	the road gradient (%)
g	the acceleration of gravity (m/s^2)
v_m	the headwind into the vehicle (m/s)
ρ_a	the air density (kg/m^3)
$v_1(t)$	the speed of the non-following vehicle at the intersection at time t (m/s)
$a_1(t)^+$	the acceleration of the non-following vehicle at the intersection at time t (m/s^2)
$a_1(t)^-$	the deceleration of the non-following vehicle at the intersection at time t (m/s^2)
vol	the road section speed of arriving vehicles (m/s)
T	the study period (h)
C	The signal cycle (s)
η	the green signal ratio
q	the vehicle arrival rate at the inbound approach (pcu/h)
ε	the velocity decrease magnitudes of the vehicle (m/s)

References

1. Wei, B.; Yagita, H.; Inaba, A.; Sagisaka, M. Urbanization impact on energy demand and CO_2 emission in China. *J. Chongqing Univ. Engl. Ed.* **2003**, *2*, 46–50.
2. Dong, Y.; Xu, J.; Liu, X.; Gao, C.; Ru, H.; Duan, Z. Carbon Emissions and Expressway Traffic Flow Patterns in China. *Sustainability* **2019**, *11*, 2824. [CrossRef]
3. Dias, D.; Antunes, A.; Tchepel, O. Modelling of Emissions and Energy Use from Biofuel Fuelled Vehicles at Urban Scale. *Sustainability* **2019**, *11*, 2902. [CrossRef]
4. Zhao, J.; Liu, Y.; Di, D. Optimization model for layout and signal design of full continuous flow intersections. *Transp. Lett.* **2016**, *4*, 194–204. [CrossRef]
5. Wu, L. Analysis and Control Methods in Vehicular Fuel Consumption on Intersections of Urban Roads. Ph.D. Thesis, Northeast Forestry University, Harbin, China, 2016.
6. Liao, T.; Machemehl, R. Development of an aggregate fuel consumption model for signalized intersections. *Transp. Res. Rec. J. Transp. Res. Board* **1998**, *1641*, 9–18. [CrossRef]
7. Liao, T. A fuel-based signal optimization model. *Transp. Res. Part D* **2013**, *23*, 1–8. [CrossRef]
8. Li, X.; Li, G.; Pang, S.; Yang, X.; Tian, J. Signal timing of intersections using integrated optimization of traffic quality, emissions and fuel consumption: A note. *Transp. Res. Part D* **2004**, *5*, 401–407. [CrossRef]
9. Lv, J.; Zhang, Y. Effect of signal coordination on traffic emission. *Transp. Res. Part D* **2012**, *2*, 149–153. [CrossRef]
10. Lv, J.; Zhang, Y.; Zietsman, J. Investigating emission reduction benefit from intersection signal optimization. *J. Intell. Transp. Syst.* **2013**, *3*, 200–209. [CrossRef]
11. Gao, Y.; Hu, H. Estimation of Queued Vehicle Emissions at Signalized Intersections Based on Vehicle Specific Power Approach. *China J. Highw. Transp.* **2015**, *4*, 101–108.
12. Zhang, Y.; Chen, X.; Zhang, X.; Song, G.; Hao, Y.; Yu, L. Assessing Effect of Traffic Signal Control Strategies on Vehicle Emissions. *J. Transp. Syst. Eng. Inf. Technol.* **2009**, *1*, 150–155. [CrossRef]
13. Tang, T.; Yi, Z.; Lin, Q. Effects of signal light on the fuel consumption and emissions under car-following model. *Phys. A Stat. Mech. Appl.* **2017**, *469*, 200–205. [CrossRef]
14. Brackstone, M.; Mcdonald, M. Car-following: A historical review. *Transp. Res. Part F* **1999**, *4*, 181–196. [CrossRef]
15. Newell, G. Memoirs on highway traffic flow theory in the 1950s. *Oper. Res.* **2002**, *1*, 173–178. [CrossRef]
16. Gazis, D. *The Origins of Traffic Theory*; INFORMS: Linthicum, MD, USA, 2002.
17. Reuschel, A. Fahrzeugbewegungen in der Kolonne. *Osterr IngenArchiv.* **1950**, *4*, 193–215.
18. Pipes, L. An operational analysis of traffic dynamics. *J. Appl. Phys. A* **1953**, *3*, 274–281. [CrossRef]
19. Chandler, R.; Herman, R.; Montroll, E. Traffic dynamics: Studies in car following. *Oper. Res.* **1958**, *2*, 165–184. [CrossRef]
20. Herman, R.; Montroll, E.; Potts, R.; Rothery, R. Traffic dynamics: Analysis of stability in car following. *Oper. Res.* **1959**, *1*, 86–106. [CrossRef]
21. Gazis, D.; Herman, R.; Rothery, R. Nonlinear follow-the-leader models of traffic flow. *Oper. Res.* **1961**, *9*, 545–567. [CrossRef]
22. Newell, G. Nonlinear effects in the dynamics of car following. *Oper. Res.* **1961**, *2*, 209–229. [CrossRef]
23. Bando, M.; Hasebe, K.; Nakayama, A.; Shibata, A.; Sugiyama, Y. Dynamical model of traffic congestion and numerical simulation. *Phys. Rev. E* **1995**, *2*, 1035–1042. [CrossRef]
24. Helbing, D.; Tilch, B. Generalized force model of traffic dynamics. *Phys. Rev. E* **1998**, *1*, 133–138. [CrossRef]
25. Jiang, R.; Wu, Q.; Zhu, Z. Full velocity difference model for a car-following theory. *Phys. Rev. E* **2001**, *64*, 017101. [CrossRef] [PubMed]
26. Wang, D.; Jin, S. Review and Outlook of Modeling of Car Following behavior. *China J. Highw. Transp.* **2012**, *1*, 115–127.
27. Ahn, K. Microscopic Fuel Consumption and Emission Modeling. Master's Thesis, Virginia Polytechnic Institute and State University, Blacksburg, VA, USA, 1998.
28. Ahn, K.; Rakha, H.; Trani, A.; Van Aerde, M. Estimating vehicle fuel consumption and emissions based on instantaneous speed and acceleration levels. *J. Transp. Eng.* **2002**, *2*, 182–190. [CrossRef]
29. Yu, S.; Shi, Z. An improved car-following model considering headway changes with memory. *Phys. A Stat. Mech. Appl.* **2015**, *421*, 1–14. [CrossRef]

30. Mamouei, M.; Kaparias, I.; Halikias, G. A framework for user- and system-oriented optimisation of fuel efficiency and traffic flow in Adaptive Cruise Control. *Transp. Res. Part C* **2018**, *92*, 27–41. [CrossRef]
31. Zhang, X.; Jia, B.; Jiang, R. Impact of safety assistance driving systems on oscillation magnitude, fuel consumption and emission in a car platoon. *Phys. A Stat. Mech. Appl.* **2018**, *505*, 995–1007. [CrossRef]
32. Li, X.; Cui, J.; An, S.; Parsafard, M. Stop-and-go traffic analysis: Theoretical properties, environmental impacts and oscillation mitigation. *Transp. Res. Part B* **2014**, *1*, 319–339. [CrossRef]
33. Abou-Senna, H.; Radwan, E.; Westerlund, K.; Cooper, C. Using a traffic simulation model (vissim) with an emissions model (moves) to predict emissions from vehicles on a limited-access highway. *J. Air Waste Manag. Assoc.* **2013**, *7*, 819–831. [CrossRef]
34. Li, J.; Wu, G.; Zou, N. Investigation of the impacts of Signal Timing on Vehicle Emissions at an isolated intersection. *Transp. Res. Part D* **2011**, *5*, 409–414. [CrossRef]
35. Jiménez-Palacios, J. Understanding and Quantifying Motor Vehicle Emissions with Vehicle Specific Power and TILDAS Remote Sensing. Ph.D. Thesis, Universidad de Zaragoza, Zaragoza, Spain, Université de Technologie de Compiègne, Compiègne, France, 1999.
36. Epa, U.S. Methodology for Developing Modal Emission Rates for EPA's Multi-Scale Motor Vehicle and Equipment Emission System. Available online: https://permanent.access.gpo.gov/lps71724/420r02027.pdf (accessed on 15 July 2019).



© 2019 by the authors. Licensee MDPI, Basel, Switzerland. This article is an open access article distributed under the terms and conditions of the Creative Commons Attribution (CC BY) license (http://creativecommons.org/licenses/by/4.0/).